

We are IntechOpen, the world's leading publisher of Open Access books Built by scientists, for scientists

6,900

Open access books available

186,000

International authors and editors

200M

Downloads

Our authors are among the

154

Countries delivered to

TOP 1%

most cited scientists

12.2%

Contributors from top 500 universities



WEB OF SCIENCE™

Selection of our books indexed in the Book Citation Index
in Web of Science™ Core Collection (BKCI)

Interested in publishing with us?
Contact book.department@intechopen.com

Numbers displayed above are based on latest data collected.
For more information visit www.intechopen.com



Autowave Processes in Magnetic Fluid: Electrically Controlled Interference

*Vladimir S. Chekanov, Natalya V. Kandaurova,
Viktoria I. Drozdova, Galina V. Shagrova,
Veniamin V. Romantsev and Mikhail Yu. Shevchenko*

Abstract

The chapter considers autowaves that were observed in the thin near-electrode layer of concentrated magnetic fluid. Autowave process is a unique object for the study of self-organization. We observed pacemakers (leading centers), reverberators (spiral waves), and wave diffraction. A mechanism for the appearance of an autowave process has been developed; its mathematical model has been proposed and realized by means of computer simulation. As a basic method of observation, we used electrically controlled interference. This method watches the changes in the spectrum of reflected light from a two-layer structure with variable thickness: “conductive ITO coating—a layer of concentrated magnetic fluid” in an electric field.

Keywords: interference, magnetic fluid, reflection, thin membrane, near-electrode layer, autowaves, pacemaker, reverberator, self-organization

1. Introduction

In this chapter, we describe a new active excitable medium—a thin near-electrode layer of magnetic fluid. The uniqueness of this environment lies in the fact that its electrophysical and optical properties can be controlled using a weak electric field. In addition, in a layer of concentrated magnetic fluid, we were able to observe and investigate the autowave process. Also, with the help of external periodic effects, it was possible to achieve synchronization of autowaves. While working on this chapter, we studied the latest innovative work on ferrofluids and modeling the processes occurring in them [1–3].

A unique phenomenon that we observed in the near-electrode layer of a magnetic fluid is an autowave process. The best known is the autowave process in the Belousov-Zhabotinsky reaction, when the color of the solution changes periodically. In nature, the autowave process is a change of predator–prey populations. In human body, autowaves spread in the heart muscle and the retina. Interest in the study of autowave processes is primarily due to the fact that in chemical, biological systems, neural networks, and the human brain, they follow the same rules of propagation [4].

We managed to observe an autowave process (Video 1 available at <https://yadi.sk/i/rUBv-Mx12DqFLQ>) in a thin near-electrode layer of a magnetic fluid (MF) placed between two electrodes in an electric field [5, 6].

The uniqueness of the experiments is that autowaves can be observed in laboratory conditions with the help of simple equipment, including transient processes and synchronization (Video 2 available at <https://yadi.sk/i/-9l5aXD5aT3tKA>). The purpose of this chapter is to study the autowave process in the near-surface layer of a magnetic fluid at the boundary with an electrode and to describe the physical model and the autowaves' appearance mechanism. Also, the goal of the chapter is to create a mathematical model and obtain its solution in the environment of modeling physical processes COMSOL Multiphysics 5.2.

2. Materials and methods

Magnetizing liquid media—magnetic fluids—is colloidal solutions of ferromagnetic particles in a liquid (kerosene, water). In our experiments, we used a liquid like “magnetite in kerosene” [7]. The typical particle size is 10 nm, which corresponds to the single-domain state in such particles and determines the superparamagnetic behavior of these systems. A surfactant (*Hol* in our experiments) is used to prevent particles from coagulating. Oleic acid creates a stabilizing layer that compensates for the dipole-dipole attraction between the magnetic particles. The thickness of the stabilizing layer is 1–2 nm. The magnetic fluid that we used in the experiments has a concentration of 3.2 vol.%, dielectric constant $\epsilon = 2.1$, and conductivity $\sigma = 3.8 \times 10^{-7} (\Omega \cdot \text{m})^{-1}$ (measured at 1000 Hz).

The autowave process observation is described below. The experiment was carried out on the unit shown in **Figure 1**.

The magnetic fluid (1) is placed into a cell between two electrodes (2, 5), made of glass with a conductive transparent coating InSnO_2 (ITO). The area of electrode surface is $S = 30 \times 40 \text{ mm}^2$ with the glass thickness of 4 mm and conductive coating thickness of $h_0 = (160 \pm 5) \text{ nm}$; the thickness of magnetic fluid first layer is 1–40 μm . A beam from a source of white light (8) falls on the surface of a cell with a magnetic fluid. The falling rays were reflected from the “electrode-magnetic liquid” border and were recorded by a camera (7). A constant or pulse voltage was applied to the electrodes (9). The prism (6) was used to separate the rays that reflected from

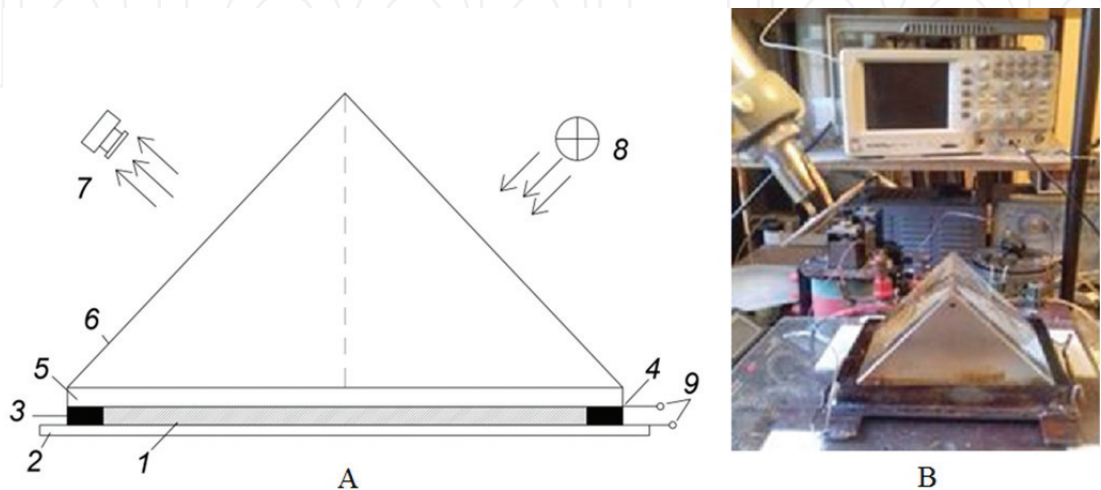


Figure 1.
(A) Schematic drawing of the experimental unit: (1) “magnetite in kerosene” magnetic fluid; (2, 5) glass with conductive coating; (3, 4) insulating gaskets; (6) prism; (7) camera or photodiode; (8) lighting (white or monochromatic light); (9) electrodes. (B) Photo of the experimental unit.

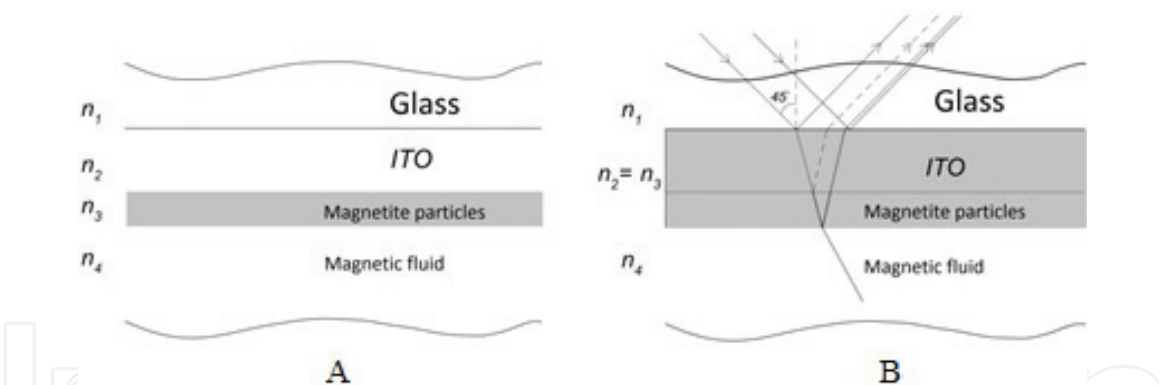


Figure 2. Model of a multilayer structure at the cell surface. (A) Model of a multilayer structure “glass – ITO – layer of magnetite particles – magnetic fluid.” (B) Model of three optical layers “glass – ITO + a layer of magnetite particles – magnetic fluid” with reflected rays.

the surface of the glass (5) and from the surface of the transparent ITO electrode. The complex refraction indices and thickness of the conductive coating (ITO) were measured by using a spectroscopic ellipsometer SE 800 SENTECH. The refraction index of glass is $n_1 = 1.52$, and the refraction index of conductive coating is $\hat{n}_2 = 1.76(1 + 0.04i)$. The refraction index of magnetic fluid with a concentration of 3.2% vol. is $\hat{n}_4 = 1.45(1 + 0.01i)$. The rays of light with a wide range of wavelengths (white light) fall on the ITO electrode and are reflected from its upper and lower borders. Since the thickness of ITO is ~ 200 nm, the interference of the reflected rays occurs. When voltage is applied to the electrodes, the magnetite particles move to the electrodes. Thin layers of a concentrated magnetic fluid (~ 27 – 30%) are formed near the electrodes, which corresponds to the dense packing of particles with a protective coating. The MF refraction index of such concentration is $\hat{n}_3 = 1.76(1 + 0.03i)$.

The refraction indices of ITO and near-electrode layer are close in value: $n_2 \approx n_3$. Therefore, the growth of near-electrode layer of concentrated magnetic fluid in the electric field is optically equivalent to the increase of conductive coating (ITO) thickness. The interference of falling rays is taking place in two-layer structure —“conductive ITO coating—a near-electrode layer.” It can be visually observed by changing of the cell surface color from green to crimson. We called this electrooptical effect as electrically controlled interference (**Figure 2**).

Depending on the near-electrode layer thickness, the surface of a cell with a magnetic fluid changed its color. The visible color change of the layer is explained by the shift of spectrum maximum due to the increase of the structure “conductive ITO coating – near-electrode layer” optical thickness. If the voltage on electrodes is more than critical voltage (~ 12 V), particles in the near-electrode layer become unstable, and the autowave process (AW-process) starts [6].

In our experiments, we considered the temperature of the liquid to be the same and did not take into account the heating during the passage of electric current and heat transfer [8].

3. Experimental results

3.1 Excitation autowave spreading modes

3.1.1 “Fast” autowave mode

A technique for the calculation of the near-electrode layer thickness is presented in [9]. Depending on the cell voltage applied to the electrodes, the thickness of the

layer varies up to 100 nm. The specific resistance of this thickness layer is several orders of magnitude greater than the specific resistance of the liquid in the cell (the thickness of the liquid layer in the cell is $\approx 40\text{ }\mu\text{m}$). Hence, the field strength at a steady-state current in a layer of such thickness also will be several orders of magnitude greater. At some critical voltage on the electrodes, the tension in the layer becomes $\sim 10^7\text{ V/m}$, and it becomes conductive (Wien effect). Individual elements (ensembles of particles) get the same charge from the electrode and move away from it. A running wave is visible on the surface of the cell (**Figure 3**).

Note that complete information about the autowave structure evolution can be obtained by describing only the time evolution of the wave front position. This is the basis for the kinematic approach to the description of autowave structures [10]. Since the cell has dimensions of $3 \times 4\text{ cm}$, we can estimate the average velocity of the wave front motion. Approximately 0.25 s passes from the appearance of green color areas (**Figure 3A**) before filling the entire surface of the cell with this color. Such wave is called “fast”; the velocity of its movement is about 16 cm/s. It looks like a flame spreading over the steppe by setting fire in different places. This is a well-known problem solved by Zeldovich and Frank–Kamenetsky.

3.1.2 “Slow” autowave mode

Further, the layer elements (ensembles of particles) fall into the cell, break apart, and lose the same charge as the electrode. They get oppositely charged in the cell and begin their movement to the electrode due to electro- and dipolar phoresis. Behind the first wave follows the second one; on the surface of the cell, there appears a picture of the autowave process (**Figure 4**). The waves move with a velocity of $\approx 1\text{ cm/s}$. These are the so-called phase (“slow”) autowaves. That is, the MF near-electrode layer is an excitable medium with a restoration. An example of such a process can be watched on video (Video 3 available at <https://yadi.sk/i/WR1vDK5IzGGxLg>).

3.2 Spiral waves (reverberators)

We managed to observe the appearance and development of spiral waves (reverberators) in the near-electrode layer of magnetic fluid (Video 4 available at

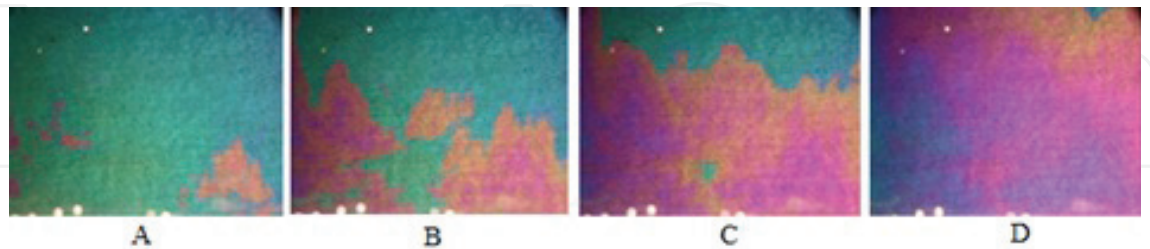


Figure 3.
“Fast” wave in the near-electrode layer of a cell with magnetic fluid.

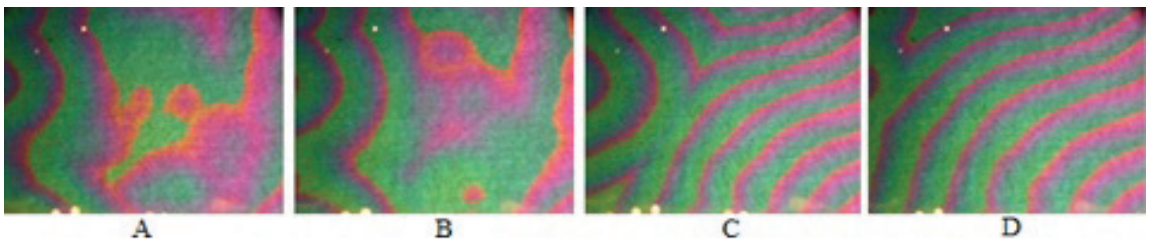


Figure 4.
Phase (“slow”) autowaves in the near-electrode layer of a cell with magnetic fluid.

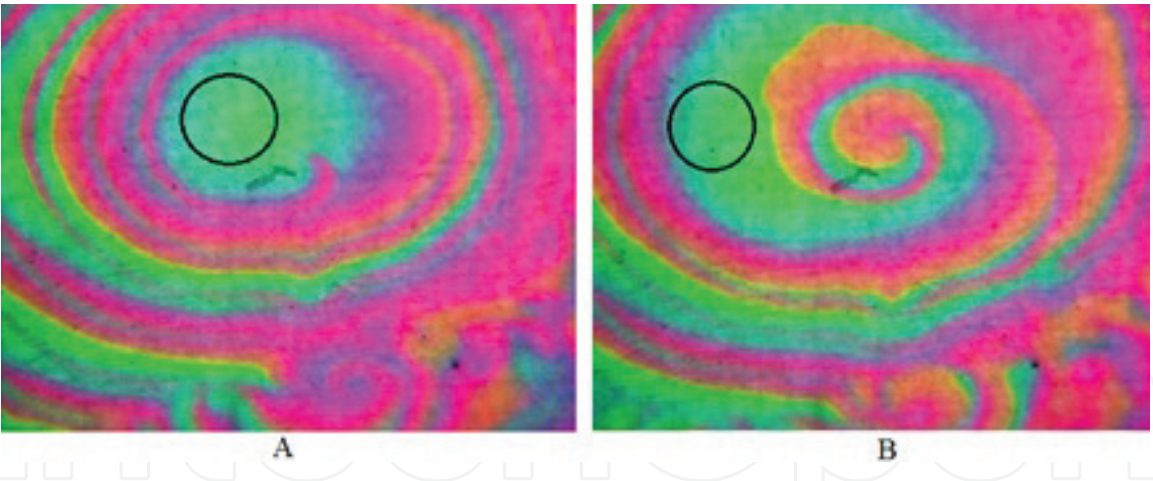


Figure 5.
Spiral waves: reverberators in the autowave process. (A) Reverberator at the beginning of the rotation period, and (B) reverberator at half of the rotation period. Singular domains are marked.

<https://yadi.sk/i/8OcbP4y831nPMQ>). These were single reverberators (**Figure 5**) and multiple ones (**Figure 6**). The reverberator’s lifetime is limited to a few turns. If several reverberators appear in the observation field, then after 20 s, only one remains [11].

Figure 5 shows a photograph of the reverberator: (A) the beginning of the reverberator rotation period and (B) half of the period. As seen in the figure, there is a region in the center of the reverberator core, corresponding to the interference pattern of reflection from the electrode at a constant layer thickness. So in this region, there is no oscillation of the layer. This is the so-called singular domain. Its existence comes from the reasoning described in [12].

3.3 Leading centers (pacemakers)

Figure 7 shows the pacemaker (leading center), which we observed in the considered active medium. Pacemakers can emit waves with different periods, as can be seen in **Figure 7A** and **B**. The larger the radius of curvature of the cylindrical wave, the lower the speed of the wave. So in **Figure 7A**, the period of the wave emitted by the pacemaker is 0.31 s. Since all characteristics in the autowave process are determined by the system itself, the period of the waves emitted by each

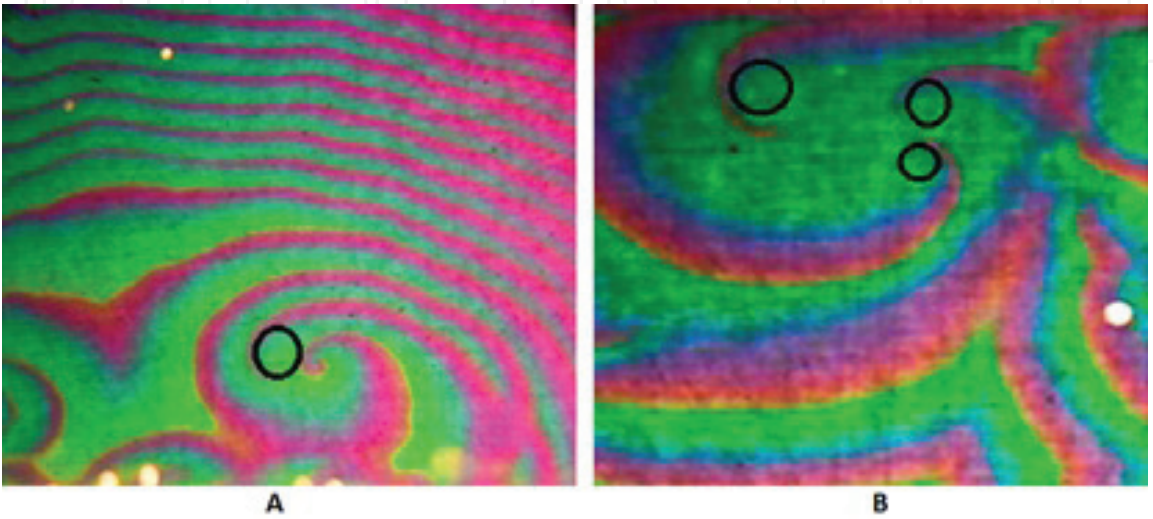


Figure 6.
(A) Two-arm reverberator and (B) three-arm reverberator. Singular domains are marked.

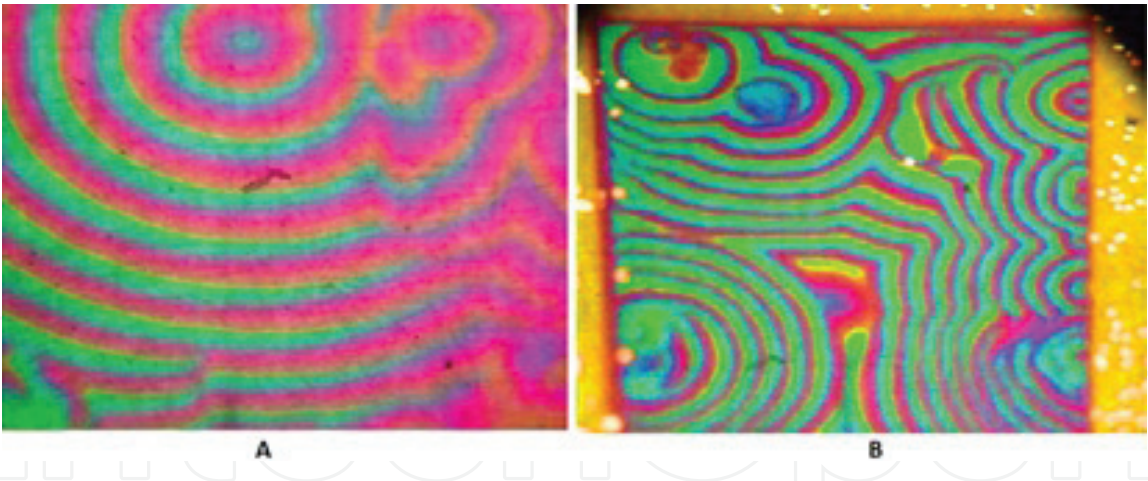


Figure 7
Experiment: pacemakers with different periods. Frame width, 1.2 cm.

pacemaker is determined only by its own properties and cannot be adjusted by external influence.

3.4 Autowave diffraction on an obstacle

Autowave is a special kind of wave that does not have standard wave properties. Autowaves do not interfere and do not transfer energy. For autowaves, the principle of superposition is not valid; they mutually destroy each other in a collision (a wave with a smaller period “destroys” a slower wave). The only common property of autowaves with conservative waves is diffraction or rounding of the obstacle. The bending of autowave near the obstacle in a cell with magnetic fluid is shown in **Figure 8**.

3.5 Propagation of autowaves in a medium with local heterogeneity: simulation of cardiac pathology

Local heterogeneity was created in the near-electrode layer of the magnetic fluid cell, as shown in **Figure 9**. This figure also shows the propagation of the autowave, which shows that there is a region around the heterogeneity and the oscillations which occur with a phase different from the oscillations of the cell surface. In this case, the current waveform has the form shown in **Figure 10**.

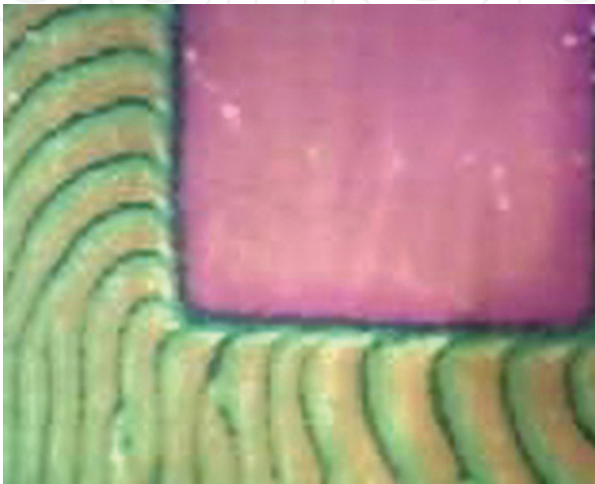


Figure 8.
Experiment: the autowave diffraction around the obstacle. Frame width, 1.2 cm.

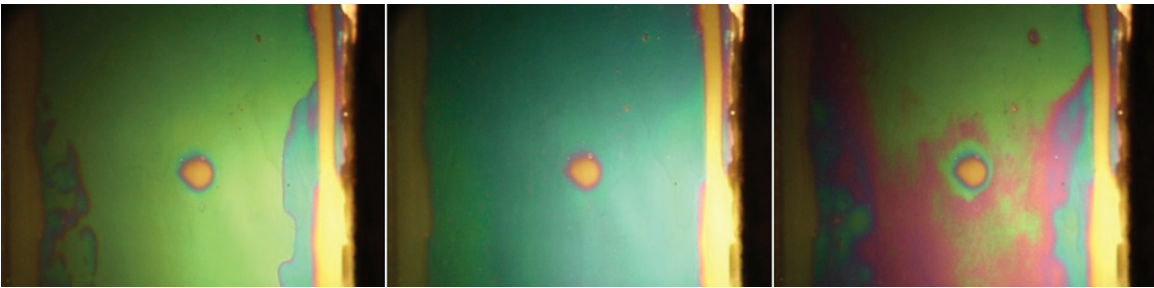


Figure 9.
Propagation of autowaves in a medium with local heterogeneity.

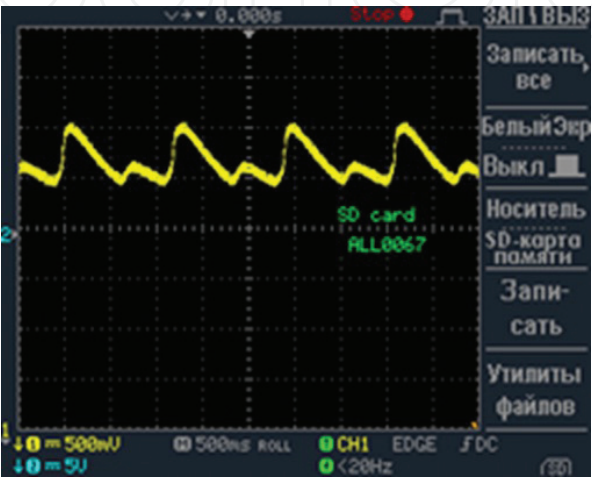


Figure 10.
Oscillogram of relaxation oscillations of a current in a cell with local heterogeneity.

We assume that the region around the local inhomogeneity has a refractoriness time R_1 , different from the refractoriness time R_2 of the medium. Therefore, the wave front reaches the section with refractoriness R_1 and gets broken. Thus, arrhythmia occurs in oscillations between the surface of the cell as a whole and the area around the local heterogeneity.

If there is a heterogeneity in the myocardium (muscle middle layer) of the heart, for example, a heart attack, which means that there is no blood supply in some area, then a similar rhythm transformation may occur in the heart muscle.

This experiment can be used as a model for processes occurring in the myocardium.

4. The physical model of the autowave process

The physical mechanism of the autowave process in the near-electrode layer of a magnetic fluid is the following: as mentioned earlier, in an electric field, the charged particles of magnetite due to electro- and dipolar phoresis move to the nearest electrode and form a close-packed layer 0–170 nm thick around it (**Figure 11**).

A thin layer—the so-called structural-mechanical barrier—appears between the layer of particles and the electrode. It consists of a dielectric—a mixture of kerosene and oleic acid molecules (surfactant surrounding the magnetite particles). The thickness of this barrier is about 10 nm, but it prevents the particle discharge because of the contact with the electrode. With the growth of the near-electrode layer, the intensity increases in the barrier. At its critical value $E \sim 10^7$ V/m, the dielectric becomes conductive and magnetite particles get recharged and start moving from the electrode—a single flat autowave passes.

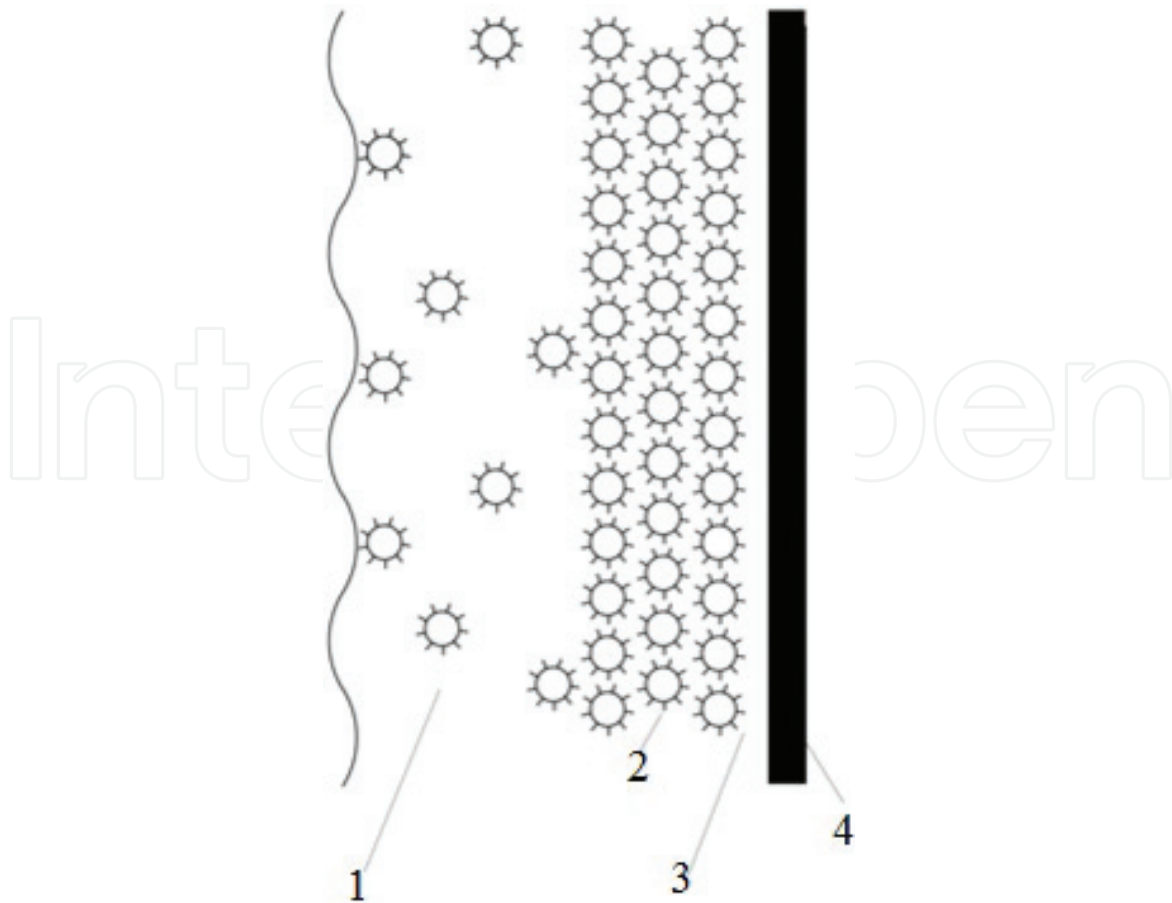


Figure 11. Schematic of a cell with a magnetic fluid with a formed near-electrode layer. (1) Magnetic fluid in the cell, (2) a layer of magnetite particles, (3) dielectric (structural-mechanical barrier), and (4) electrode (ITO).

We assume that the medium is excitable and that it consists of a set of elementary areas of near-electrode layer. According to definition, each such site is an autonomous source of energy. Energy is accumulated due to the so-called polarization capacitance of near-electrode layer of particles [13]. The elements of an excitable medium interact with each other, transferring the energy of electrical and hydrodynamic interaction from one to another. This is how the excitation pulse transmits. This process is similar to the interaction of nonlinear coupled oscillators with a short coupling, where each oscillator is associated with only several adjacent ones. Thus, the physical meaning of the autowave process mechanism considered by us is a system of coupled nonlinear oscillators.

An excitable element has only one stable stationary state. An external impact that exceeds the threshold level can take an element out of a steady state and make it take action before it returns to that state. During the action, the active element can affect the elements associated with it and, in turn, remove them from the stationary state. As a result, an excitation wave propagates in such a medium. This is the most common type of autowaves in biological systems such as nerve tissue or heart muscle. In our medium, each section of the near-electrode layer affects the neighboring areas, transferring the charge and thereby removing them from the equilibrium state.

The element of an excitable medium can be in three states—rest, excitation, and refractoriness.

The local elements that make up the active medium under study (elements of the near-electrode layer) have “the only distinguished state of rest that is stable with respect to fairly weak external influences” [13]. This is a state of the medium, when

the electrode layer has already formed, (the voltage on the electrodes is less than the critical one), but the autowave process has not yet begun.

When the voltage on the electrodes exceeds critical, the element gets excited and becomes active, and a discharge occurs in the elementary capacitor. This is the state of excitation or the so-called active transition, after which the elementary segment of the layer disappears, because the layer in this local region is destroyed. In this case, a single wave front passes over the surface.

Refractoriness is a state that comes after excitation when the medium accumulates energy and cannot produce a new impulse. The medium must restore its properties with the energy coming from outside and prepare for the next impulse. The energy from the external source continues to flow, and the magnetite particles move to the nearest electrode, forming a system of successively connected capacitors: first electrode – structural-mechanical barrier – the layer of close-packed particles – magnetic fluid of low concentration – the layer of close-packed particles – structural-mechanical barrier – second electrode. The period of refractoriness corresponds to the charging of capacitors, one plate of which is an electrode and the other is near-electrode layer.

5. Synchronization of the autowave process under the influence of a periodic electric signal

In this section, we describe the synchronization of an autowave process by an external influence in a thin near-electrode layer of a magnetic fluid.

One of the main trends in the living world is the tendency to achieve a common rhythm in collective behavior—a tendency toward synchronization. An example of synchronization in nature is a colony of simultaneously flashing fireflies; these are simultaneously flapping birds flying in a flock. In technics, synchronization is important when designing computers with parallel architecture.

It was also noted that the most famous example of an active autowave environment is the Belousov-Zhabotinsky chemical reaction. Petrov et al. [14] experimented with the photosensitive form of such a reaction using periodic optical effects.

Earlier we noted that the autowave process in the near-electrode layer of magnetic fluid is considered from the standpoint of oscillations of coupled oscillators. Each element of the layer (an ensemble of particles) interacts with its nearest neighbors or, in a more complicated case, with several neighbors.

Each oscillator oscillates with its own frequency, but also we could see oscillator clusters that oscillated with the same frequency.

We affected the self-oscillation medium (oscillators) with an external periodic force (pulsed electric field) and achieved synchronization. As the synchronization criterion, the conditions of frequency and/or phase adjustment are used. It is considered that the oscillator 1:1 is synchronized by an external periodic effect, if its own frequency f_0 becomes equal to the frequency of the external signal f_e .

In addition to the criterion “frequency capture,” another criterion is used —“phase capture.” This criterion means that for any moment of time t , the condition $|f_e(t) - f_0(t) - \text{const}| < 2\pi$ is satisfied.

We affected on the observed self-oscillations in a thin near-electrode layer of magnetic fluid by a periodic pulsed electric field and selected its frequency f_e in such a way that it matched with the natural oscillation frequency of the layer elements. Thus, with a frequency capture of 1:1, we obtained a picture of autowave synchronization as shown in **Figure 12**. This picture allows us to determine the natural oscillation frequency f_0 of the elements of the near-electrode layer of magnetic fluid.

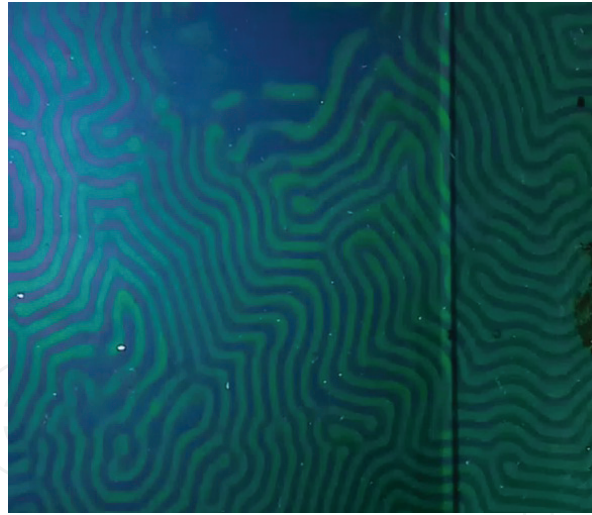


Figure 12.

Synchronization of autowaves in a thin layer of concentrated magnetic fluid by an external pulsed electric field. The ratio of the natural oscillation frequency of the elementary section of the layer f_o and the frequency of the pulsed electric field f_e is 1:1.



Figure 13.

The formation of breaks and labyrinth structures with the ratio of frequencies: $f_e \sim 2f_o$.

If the ratio of the frequency of a pulsed electric field and the natural frequency are 2:1, then a few time after the beginning of the effect, we observed breaks and labyrinth structures, as shown in **Figure 13**, or two clouds, which oscillate with a phase shift of π , as shown in **Figure 14**.

Since the near-electrode layer of magnetic fluid is a heterogeneous medium, it can be assumed that the synchronization mechanism is similar to the formation of clusters in the intestine: oscillators with similar frequencies tend to group together.

With a ratio of 1:3, three uniformly oscillating clouds were observed (**Figure 15**).

The synchronization mechanism is the following: each point tends to synchronize with external force, as well as with neighboring points. If there were no interaction in the medium, then, with a frequency ratio of about $1:m$, neighboring points would have an equal probability of the phase difference $2\pi/m$ i , where $i = 1, \dots, m^{-1}$. Because of the interaction, the points tend to have the same phases as the neighbors, and a compromise is achieved through the formation of clouds. Obviously, the phase difference between the clouds is $2\pi/m$ i [15].

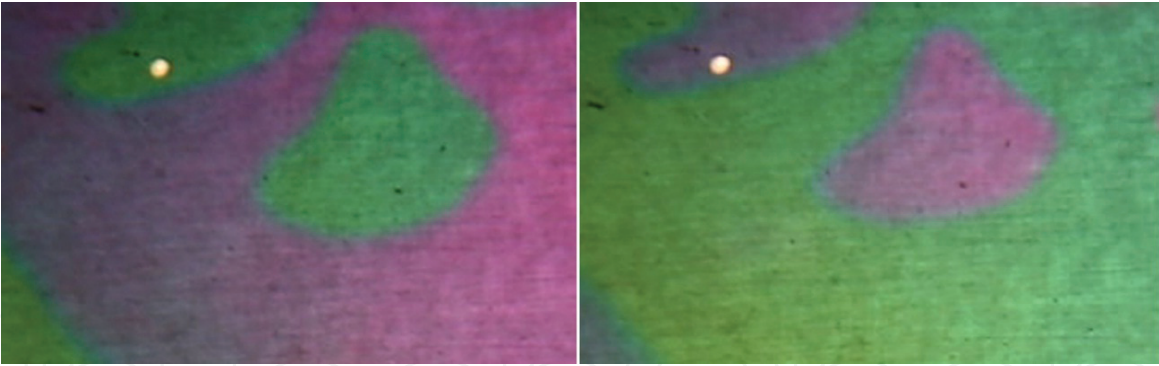


Figure 14.
Two clouds of synchronously oscillating points. The shift of phase between oscillations is π .

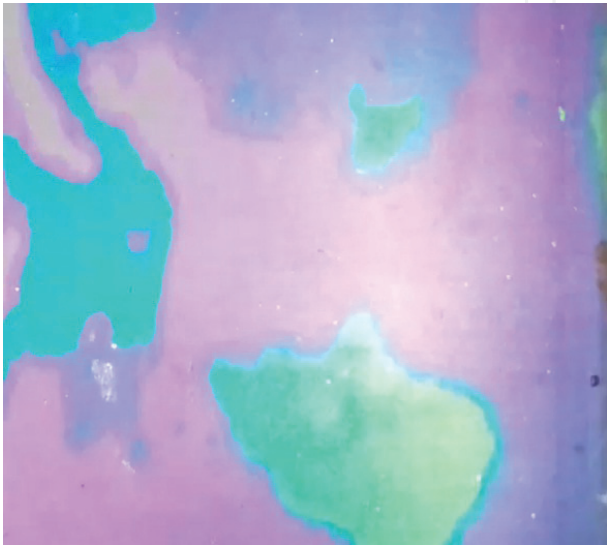


Figure 15.
Three uniformly oscillating clouds.

6. Mathematical model of the autowave process

To simulate spiral waves, pacemakers, and synchronization, we use the basic FitzHugh-Nagumo model (FHN). It describes an excitable medium and is named after Richard FitzHugh (1922–2007), who proposed the system in 1961, and Nagumo, who proposed a similar scheme the next year. It allows to adjust the characteristics of the autowave process widely and change the parameters of its behavior. Model solution can be obtained using the finite element method [16].

The model consists of two equations; the first equation describes a “fast” process—a change in the intensity in the near-electrode layer after the increase in the conductivity of the structural-mechanical barrier.

The second equation describes a slow process—the change in charge of the near-electrode layer, when charged particles of magnetite accumulate in it.

$$\begin{aligned}\frac{\partial V}{\partial t} + \frac{\partial^2 V}{\partial t^2} &= D\Delta V - V^3 + V - I \\ \frac{\partial I}{\partial t} &= \varepsilon(V + \alpha - bV)\end{aligned}\tag{1}$$

where V is the function, depending on the field intensity in a thin near-electrode layer of a magnetic fluid (activator), I is the function associated with a change in

charge (inhibitor), D is the diffusion coefficient of the activator, and ε is a small parameter; presumably this is the ratio of the time of single pulse passage and the time of the near-electrode layer formation.

Depending on the values of the parameters α and β , the medium element can be either in the oscillatory mode or in the excitable mode.

The proposed model of the autowave process was implemented by means of the COMSOL Multiphysics 5.2. The solutions that were obtained for spiral waves, pacemakers, and obstacle diffraction correspond to full-scale experiments and confirm the adequacy of the proposed model (1).

The simulation results and comparison with experimental data are shown in **Figures 16–18**.

We were able to show that the diffraction of autowaves (bending the obstacles) is a consequence of the existence of a region with nonlinear characteristics near the obstacles. One of the characteristics is the deceleration parameter φ .

The coefficient φ depends only on the distance to the nearest point of the obstacle and is calculated by the following formula:

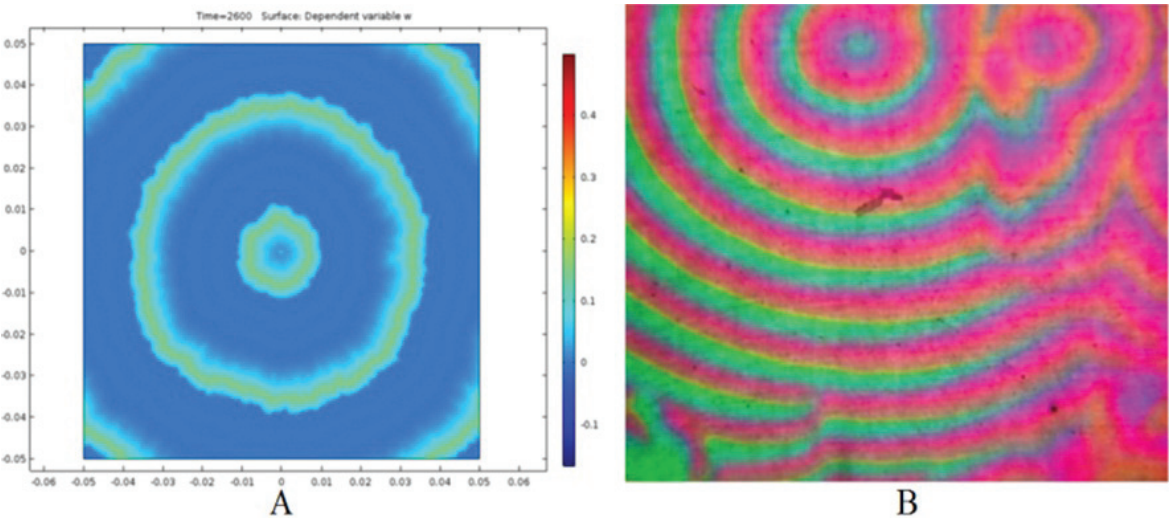


Figure 16. Comparison of the results of pacemaker simulation and experiment. (A) The result of modeling a single pacemaker; (B) the result of a full-scale experiment.

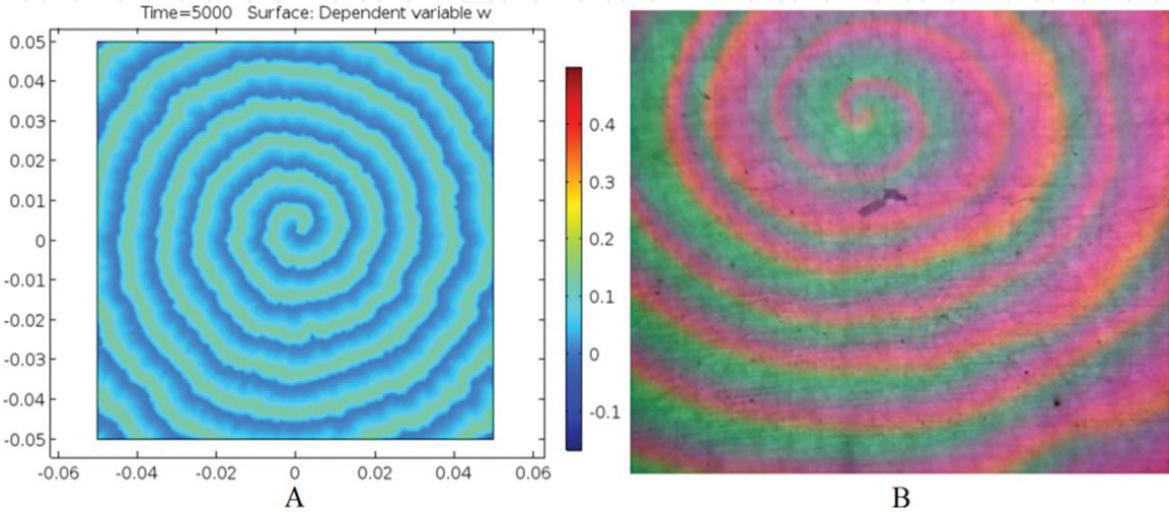


Figure 17. Comparison of the results of spiral wave simulation and experiment. (A) The result of modeling the development of a one-arm reverberator; (B) the result of a full-scale experiment.

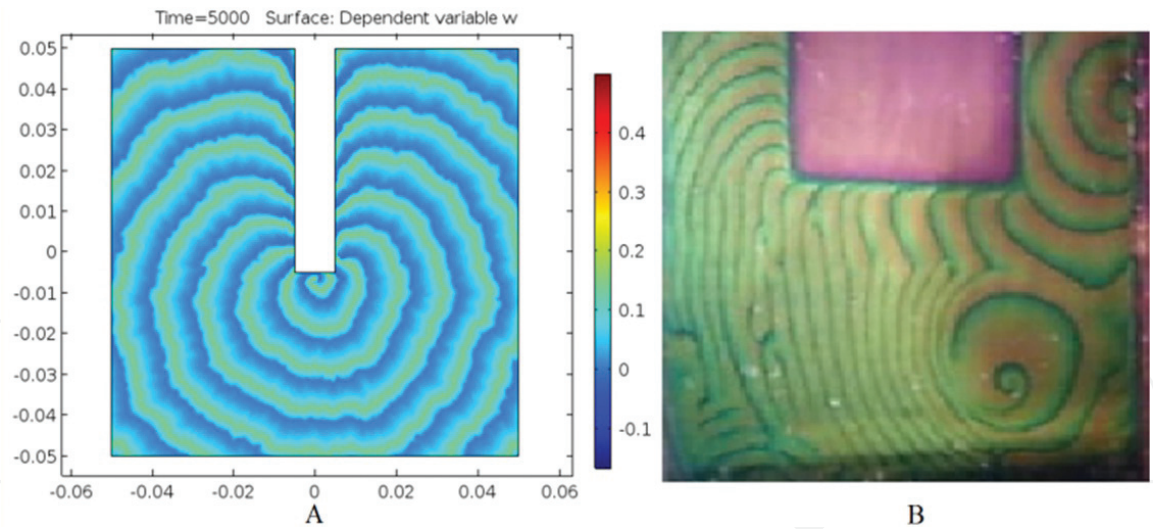


Figure 18.
Comparison of the autowave diffraction simulation results and experiment: (A) modeling the rounding of an obstacle; (B) the result of a full-scale experiment.

$$\varphi = \left(\frac{d}{r}\right)^4 * H(d < r) \tag{2}$$

where d is the distance to the obstacle, r is the range of the deceleration function, and H is the Heaviside function.

7. Conclusions

This chapter describes the study of the autowave process in a layer of concentrated magnetic fluid that forms at the electrode in an electric field. The main modes of the autowave process are investigated: pacemakers and reverberators (spiral waves) and obstacle rounding (autowave diffraction). All visualizations are obtained by the author’s method of electrically controlled interference in a thin layer.

The uniqueness of the medium we study is that the autowave process is controlled by a weak electric field. It can be observed indefinitely, and this process is easily reproduced in the laboratory. Also synchronization by external influence was studied in the electrically controlled medium.

We consider very important to investigate and control heterogeneities (obstacles) in the active medium. Heterogeneities are the main reason that causes the development of cardiac arrhythmias and heart attacks in the human heart. By controlling the movement of a wave around a heterogeneity, arrhythmia can be eliminated. This is important for practical use.

A mathematical model of the autowave process, based on the FitzHugh-Nagumo basic model, is created for the near-electrode thin layer of a magnetic fluid. The model is implemented in the interactive environment for physical processes simulation—COMSOL Multiphysics 5.2. The coefficients in the equations of the modified FHN system are found; using these coefficients, we can simulate different autowave modes.

A criterion for the adequacy of the model is a visual correspondence to the full-scale experiment.

All the features of the formation and propagation of reverberators, pacemakers, and diffraction in the autowave medium observed in the natural experiment are

repeated in computer simulation, which will allow us to find further methods for controlling the development of autowave process. This has practical application either in fundamental field or in practical purposes.

Acknowledgements

This paper was written as part of the state task Project No 3.5385.2017/8.9 for the implementation of the project on the topic: “Experimental research and mathematical modeling of interphase and near-surface phenomena in a thin membrane of nanostructured magnetic fluid” in MIREA—Russian Technological University.

Thanks

Authors give their great thanks to Prof. Chekanov V.V. (RIP) for the invaluable help in preparing the materials and experimental results.

Author details

Vladimir S. Chekanov¹, Natalya V. Kandaurova^{1*}, Viktoria I. Drozdova², Galina V. Shagrova², Veniamin V. Romantsev³ and Mikhail Yu. Shevchenko⁴

¹ MIREA—Russian Technological University, Stavropol Branch, Stavropol, Russia


² North-Caucasian Federal University, Stavropol, Russia

³ St. Petersburg State Electrotechnical University “LETI” named after V.I. Ulyanov (Lenin), St. Petersburg, Russia

⁴ Wonder Technologies LLC, Moscow, Russia

*Address all correspondence to: candaur18@yandex.ru

IntechOpen

© 2019 The Author(s). Licensee IntechOpen. This chapter is distributed under the terms of the Creative Commons Attribution License (<http://creativecommons.org/licenses/by/3.0>), which permits unrestricted use, distribution, and reproduction in any medium, provided the original work is properly cited. 

References

- [1] Sheikholeslami M, Barzegar Gerdroodbary M, Moradi R, Shafee A, Li Z. Application of neural network for estimation of heat transfer treatment of $\text{Al}_2\text{O}_3\text{-H}_2\text{O}$ nanofluid through a channel. *Computer Methods in Applied Mechanics and Engineering*. 2019;**344**: 1-12
- [2] Sheikholeslami M. Numerical approach for MHD Al_2O_3 -water nanofluid transportation inside a permeable medium using innovative computer method. *Computer Methods in Applied Mechanics and Engineering*. 2019;**344**:306-318
- [3] Sheikholeslami M. New computational approach for exergy and entropy analysis of nanofluid under the impact of Lorentz force through a porous media. *Computer Methods in Applied Mechanics and Engineering*. 2019;**344**:319-333
- [4] Zaikin AN, Zhabotinsky AM. Concentration wave propagation in two-dimensional liquid-phase self-oscillating system. *Nature*. 1970;**225**: 535-537
- [5] Chekanov VV, Iljuch PM, Kandaurova NV, Bondarenko EA. Autowaves in near-surface layer of magnetic fluid. *Journal of Magnetism and Magnetic Materials*. 2005;**289**: 107-109
- [6] Chekanov VV, Kandaurova NV, Chekanov VS. Phase autowaves in the near-electrode layer in the electrochemical cell with a magnetic fluid. *Journal of Magnetism and Magnetic Materials*. 2017;**431**:38-41
- [7] Rosensweig RE. *Ferrohydrodynamics*. Cambridge: Univ. Press; 1985. 344p
- [8] Sheikholeslami M, Mehryan SAM, Shafee A, Sheremet MA. Variable magnetic forces impact on magnetizable hybrid nanofluid heat transfer through a circular cavity. *Journal of Molecular Liquids*. 2019;**277**:388-396
- [9] Chekanov VV, Kandaurova NV, Chekanov VS. Thickness calculation of thin transparent conductive membrane on the border with a magnetic fluid. *Journal of Nano-and Electronic Physics*. 2016;**8**:143-148
- [10] Davydov VA, Zykov VS, Mikhailov AS. Kinematics of autowave structures in excitable media. *Advances in Physical Sciences*. 1991;**161**:45-83
- [11] Chekanov VV, Kandaurova NV, Chekanov VS. Experimental study of the properties of autowave sources (reverberators) in the magnetic fluid near-electrode layer using reflected light interference. *Magnetohydrodynamics*. 2017;**53**(3):495-500
- [12] Ivanitsky GR, Krinsky VI, Selkov EE. *Mathematical Biophysics of the Cell*. Moscow: Science Publ. House; 1978. p. 308
- [13] Kandaurova NV, Chekanov VV, Chekanov VS. Effect of a near-surface nanolayer formation on the magnetic fluid electrical properties. *Acta Tech*. 2018;**63**(4):555-562
- [14] Petrov V, Ouyang Q, Swinney HL. Resonant pattern formation in a chemical system. *Nature*. 1997;**388**: 655-657
- [15] Pikovsky A, Rosenblum M, Kurths J. *Synchronization. A Universal Concept in Nonlinear Sciences*. Cambridge, Great Britain: Cambridge University Press. pp. 167-169
- [16] Sheikholeslami M, Haq R-u, Shafee A, Li Z. Heat transfer behavior of nanoparticle enhanced PCM solidification through an enclosure with V shaped fins. *International Journal of Heat and Mass Transfer*. 2019;**130**:1322-1342